ACS Catalysis

Research Article

pubs.acs.org/acscatalysis

Gold Supported on Graphene Oxide: An Active and Selective Catalyst for Phenylacetylene Hydrogenations at Low Temperatures

Lidong Shao,*[,†] Xing Huang,[‡,§] Detre Teschner,[§] and Wei Zhang[∥]

[†]College of Environmental and Chemical Engineering, Shanghai University of Electric Power, 2103 Pingliang Road, Shanghai 200090, P. R. China

[‡]Key Laboratory of Photochemical Conversion and Optoelectronic Materials, Technical Institute of Physics and Chemistry, Chinese Academy of Sciences, Zhongguancun East Road, 100190 Beijing, P. R. China

[§]Department of Inorganic Chemistry, Fritz-Haber Institute of the Max Planck Society, Faradayweg 4-6, 14195 Berlin, Germany

[∥]Department of Energy Conversion and Storage, Technical University of Denmark, Risø campus, Frederiksborgvej 399, 4000 Roskilde, Denmark

Supporting Information

ABSTRACT: A constraint to industrial implementation of gold-catalyzed alkyne hydrogenation is that the catalytic activity was always inferior to those of other noble metals. In this work, gold was supported on graphene oxide (Au/GO) and used in a hydrogenation application. A 99% selectivity toward styrene with a 99% conversion in the hydrogenation of phenylacetylene was obtained at 60 °C, which is 100 to 200 °C lower than optimal temperatures in most previous reports on Au catalysts. A series of gold- and palladium-based reference catalysts were tested under the same conditions for phenylacetylene hydrogenation, and the performance of Au/GO was substantiated by studying the role of functionalized GO in governing the geometrical structure and thermal stability of supported Au nanoparticles under reaction conditions.

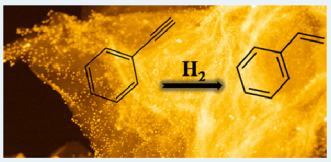

KEYWORDS: *gold, graphene oxide, phenylacetylene hydrogenation, activity, selectivity, low temperatures, low coordination sites*

In polymerization industry, styrene and ethylene feedstock usually contains small quantities (<2%) of acetylene compounds, which poison olefin polymerization catalysts. Thus, preliminary removal of alkynes via selective hydrogenation is necessary.[1,2] Despite being the most applicable catalyst in alkyne selective hydrogenation, palladium-based catalysts suffer fast deactivation and selectivity loss due to the accumulated carbonaceous deposition and the delicate subsurface chemistry under hydrogenation conditions.[3,4]

In contrast to the chemically inert nature of bulk gold, nanosized gold displays rich surface chemistry.[5,6] Alkyne-selective hydrogenation has been reported using supported gold nanoparticles (AuNPs) as catalyst materials in the last decades.[6−12] Although AuNPs exhibited high selectivities on various supporting materials, a constraint to practical applications was that the catalytic activity was always inferior to those of other noble metals. The optimal temperature windows in previous studies on gold-catalyzed alkyne hydrogenation have been commonly reported to be above 150 °C.[6−13] Thus, elevated temperature is usually required for gold-based catalyst to achieve meaningful magnitudes of reactivity. Accordingly, designing gold-based catalysts for alkyne hydrogenation with stabilized selectivity at lower temperatures is a decisive step for industrial implementations. To the best of our knowledge, gold supported on graphene or graphene oxide has rarely been reported in hydrogenation applications to date.

In the present work, phenylacetylene hydrogenation was conducted over gold supported on graphene oxide (Au/GO). Gold supported on carbon nanotubes (Au/CNTs), palladium supported on graphene oxide (Pd/GO), and palladium supported on CNTs (Pd/CNTs) were prepared and applied under the same conditions for references. Commercially available catalysts of palladium on charcoal (Pd/C) and palladium on alumina (Pd/Al_2O_3) were applied for catalytic comparisons. The morphologies of Pd/GO, Pd/C, Pd/Al_2O_3, and Pd/CNTs are shown in Figure S1 in Supporting Information (SI), where the dispersion of Pd nanoparticles is displayed for each catalyst. For comparing catalytic properties of several catalysts under the same hydrogenation conditions, the continuous flow system permits a fast optimization of reaction conditions and aids catalyst collections without filtration steps. Au/GO was studied in both continuous flow and batch systems. Other catalysts were studied in the flow system only.

Hydrogenations were carried out with a stock 0.02 M solution of phenylacetylene using ethanol as solvent. Reactant solution was pumped into the capsule of flow reactor at a flow rate of 0.2 mL/min. Each capsule carries the same amount of catalysts. At each temperature, effluent solution was collected after 15 min stabilization under reaction conditions. Each collection lasted for 3 min. After collection, the reaction temperature in the reactor was increased directly to the next

Received: March 6, 2014
Revised: June 8, 2014
Published: June 12, 2014

target, and the same procedures were repeated. After one cycle of running at 40, 60, 80, 100 °C respectively, the reactor was cooled to room temperature and washed by solvent. Such hydrogenation cycle was repeated for three times for each catalyst for evaluating the catalytic stabilities. After proper stabilizations at each temperature (15 min under reaction conditions), collected catalytic results are within 2% deviation.

Reactant conversion and selectivity values versus temperature are shown in Table 1. Full conversions were obtained at 40 and 100 °C when Pd/GO, Pd/C, Pd/Al_2O_3, and Pd/CNTs were used. Despite the various supports and metal loadings, no selectivity toward styrene was obtained for any of the Pd-based catalysts. In contrast to the Pd-based catalysts, a conversion of 5% with a selectivity of 99% toward styrene was obtained at 40 °C for Au/GO. Increasing temperature (60, 80, and 100 °C) resulted in full phenylacetylene conversion (99%) with stabilized selectivities of 99%. The estimated turnover frequency (TOF) at the applied conditions and at full conversion is 360 h^{-1}, which is consistent with a recent work[8] using gold as catalyst for phenylacetylene hydrogenations. Please note that this is the lower limit to the real TOF, because at full conversion we do not probe the kinetic regime of the catalyst. Reaction over Au/CNTs under the same conditions exhibited lower activities and selectivities at each temperature. A decrease of activity and selectivity was also observed on Au/GO that underwent prolonged reduction time during sample preparation.

Table 1. Phenylacetylene Hydrogenations over Au/GO, Au/CNTs, Pd/GO, Pd/C and Pd/Al_2O_3, and Pd/CNTs

catalysts[a,b]	temp	conversion %	styrene selectivity %[c]
Au/GO(2 wt %)	40 °C	5	99
Au/GO(2 wt %)	60 °C	99	99
Au/GO(2 wt %)	80 °C	99	99
Au/GO(2 wt %)	100 °C	99	99
Au/CNTs(2 wt %)	60 °C	75	90
Au/CNTs(2 wt %)	80 °C	80	90
Au/CNTs(2 wt %)	100 °C	95	90
Pd/GO(2 wt %)	40 °C	99	0
Pd/GO(2 wt %)	100 °C	99	0
Pd/C(1 wt %)	40 °C	99	0
Pd/C(1 wt %)	100 °C	99	0
Pd/Al_2O_3(1 wt %)	40 °C	99	0
Pd/Al_2O_3(1 wt %)	100 °C	99	0
Pd/CNTs(2 wt %)	40 °C	99	0
Pd/CNTs(2 wt %)	100 °C	99	0
Au/GO(2 wt %)[d]	60 °C	60	80
Au/GO(2 wt %)[d]	80 °C	70	80
Au/GO(2 wt %)[d]	100 °C	90	80

[a]The metal loadings of self-prepared Au/GO, Au/CNTs Pd/CNTs, and Pd/GO are measured by X-ray fluorescence analysis (XFA); Pd/C and Pd/Al_2O_3 are supplied from Sigma-Aldrich. [b]For each catalyst, the same amount (30 mg) of catalyst material was tested for hydrogenations. [c]Product mixtures were analyzed by HPLC, and no byproducts from polymerization or ethanol dehydration were detected. [d]Au supported on GO with prolonged reduction time.

The observed full-hydrogenation toward ethylbenzene on Pd/GO, Pd/C, Pd/Al_2O_3, and Pd/CNTs is consistent with reported low selectivities over monometallic Pd-based catalysts in alkyne hydrogenation.[3,13] On the other hand, achieving high activities and selectivities at 60 °C over Au-based catalysts in alkyne selective hydrogenation can be considered as a novel result as the optimal temperature window in previous studies of gold-catalyzed alkyne hydrogenation has mostly been above 150 °C.[6−13]

To confirm the improved catalysis over Au/GO in phenylacetylene selective hydrogenation, a conventional batch system was also applied (see SI for experimental details). Full conversion was obtained after 2 h at 60 °C, and high styrene selectivities were observed at the applied batch conditions (Figure S2 in SI). The same results from both continuous flow and batch systems indicate that catalyzing phenylacetylene hydrogenation with high activities and selectivities at low temperature is an intrinsic property of Au/GO.

Compared to Pd-based catalysts, significantly improved catalytic results over Au/GO at low temperatures prompted an in-depth examination of its electronic properties under reactive atmosphere. In situ X-ray photoelectron spectroscopy (XPS) was applied to study the surface and subsurface regions of catalysts. We characterized the state after storing the fresh "as-is" sample in air, as well as under H_2 at room temperature and 100 °C. The Au*4f* profiles of Au/GO (Figure 1a) exhibited metallic phases in the fresh state as well as under H_2 at room temperature and 100 °C (no surface and subsurface modification or new-phase formation were traced), whereas palladium can transform into the well-known palladium hydride under H_2 at room temperature (Figure 1b).

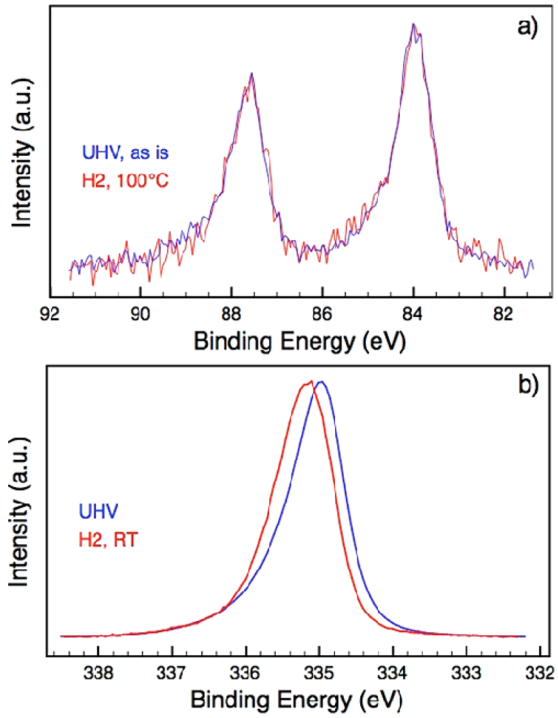

Figure 1. In situ XPS analysis of (a) Au 4f region of Au/GO in fresh (as is) status and under 1 mbar of hydrogen at 100 °C and (b) Pd 3d region of Pd foil in fresh (as is) status and under hydrogen at room temperature in the *β*-hydride state.

Subsurface chemistry governs the catalytic properties of Pd-based catalysts in selective hydrogenation applications.[3,4,14−16] Pd−hydride (PdH_x), Pd−carbide(PdC_y), or coexistence of both phases PdH_xC_y may influence catalysis by affecting and generating active phases under reaction conditions. Therefore, the activity and selectivity over Pd-based catalysts during

dx.doi.org/10.1021/cs5002724 | ACS Catal. 2014, 4, 2369−2373

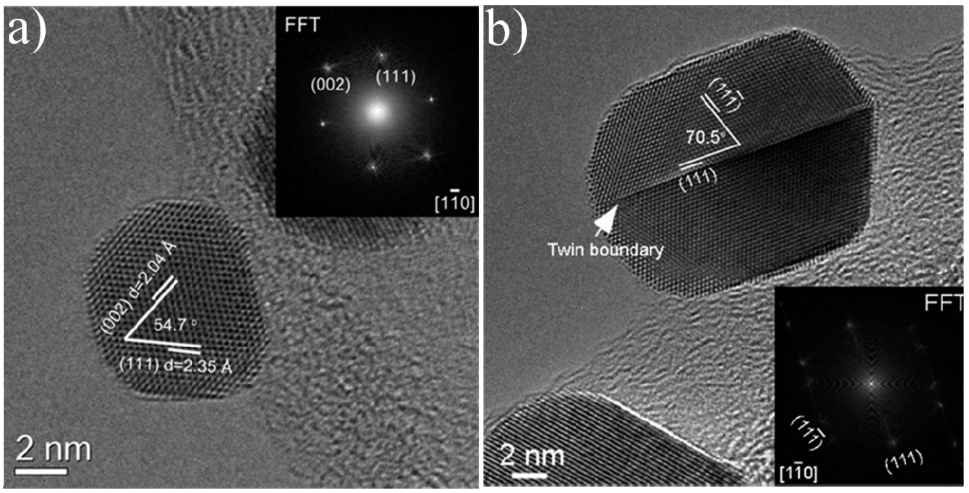

Figure 2. (a) HRTEM image of an AuNP on GO, with an inset of the fast Fourier transform. (b) HRTEM image of an AuNP on GO after prolonged reduction treatment, with an inset of the fast Fourier transform.

hydrogenations are highly dependent on the applied conditions and the catalyst prehistory. As for monometallic Pd catalysts used in the current work, full-hydrogenation took place due to the strong affinity of palladium toward H_2. As for AuNPs supported on GO, the absence of surface and subsurface dynamics indicated much weaker interaction with H_2, in line with previous DFT calculations[9] and the preferential adsorption toward C≡Cs. Moreover, the high styrene selectivity was independent of reaction temperatures, which suggests that the product readily desorbed from the catalyst without undergoing secondary hydrogenation or other side reactions. Thus, the enhanced preferences of adsorbing phenylacetylene and desorbing styrene explains the improved selectivity toward styrene over supported AuNPs on GO. In fact, the lack of styrene hydrogenation even at full phenylacetylene conversion (see Table 1 or Figure S2 in SI) suggests very weak interaction of styrene with Au/GO and/or the barrier of its further hydrogenation being far above the potential energy of styrene desorption.

Compared to Pd-based catalysts, full-hydrogenation is not favored over nanoscale gold, which is also in line to the absence of surface and subsurface dynamics of Au under reaction conditions. However, detailed analyses of active phases on Au/GO are required to interpret the obtained high activities and selectivities at much lower temperatures than previous reports. Before we investigate the geometrical structures of supported AuNPs, studying the supporting effect of GO is crucial, because it may affect the size, shape, crystalline structure, as well as the thermal stability of supported AuNPs under reactive atmosphere. CNTs, as reference materials, were applied as support of AuNPs which were tested in phenylacetylene hydrogenations under the same conditions.

Distribution and intensity of functional groups over the carbon support is proportional to the degree of surface functionalization. In the process of functionalizing carbon nanomaterials, functionalities are introduced by oxidative treatments due to their high efficiency and simplicity.[3,15,17] In the present work, strong oxidation was applied to attack and expand the graphitic layers of graphite. Consequently, the obtained GO possesses a heavily functionalized surface with large surface area. As for functionalized CNTs, one-step HNO_3 treatment has not led to a morphology change on CNTs. Microscopic analysis showed that the inner walls of the CNTs were graphitic, suggesting that the inner walls were not attacked or oxidized during the oxidation process. The XPS analysis of Au/GO and Au/CNTs (Figure S3 in SI) reflects a stronger functionalization on GO than on CNTs, the O/C ratio being 0.12 on GO and 0.06 on CNTs.

In Figure S4 in SI, a STEM image displays the well-dispersed character of AuNPs on GO with a mean particle size of 5.2 ± 0.2 nm. Some aggregates of AuNPs are also visible on a large area of GO. A close observation of a supported AuNP on GO is shown in Figure 2a; the lattice fringes (002) and (111) with a characteristic acute angle of 54.7° were identified on a rounded AuNP based on the JCPDS card (no. 04-0784) with space group $Fm\bar{3}m$. Nevertheless, the rounded AuNPs on the present GO possess enriched low coordination sites (edge, stepped, and kink) next to the exposed facets. As for Au/CNTs, high-resolution microscopic studies revealed multiply twinned Au particles (MTPs) supported on CNTs (Figure S5 in SI) with an increased mean particle size (8.4 ± 0.2 nm).

The kind of metal and the local atomic structure of the surface both affect the ease by which the hydrogen molecule becomes dissociatively chemisorbed. Over coinage metals, hydrogen dissociation is either not preferred or happens with a low rate. Sljivancanin and Hammer pointed out the importance of vacancy and kink sites for this reaction over Cu.[18] They attributed the high reactivity of these defects due to the broken Cu−Cu bridge bonds, which cause reduced Cu(4sp)-$H_2(\sigma)$ repulsion but unchanged Cu(4sp)-$H_2(\sigma^*)$ attraction. We expect the same situation for Au. Now, in general, decreasing the coordination number of surface atoms (creating steps, kink, and corners), the d-bandwidth becomes necessarily smaller.[19,20] This, in turn, shifts the d-band center toward the Fermi level. Therefore, these lower coordination sites bind adsorbates stronger than those on perfect low Miller index planes.[19,20] Because hydrocarbon adsorption of low Miller index gold facets is very weak,[9,12] this indicates that sites with low coordination number not only activate hydrogen but also play an important role in adsorbing hydrocarbon reactants. With the proper choice of support and reduction temperature, nonionic gold particles can be formed with high density of low coordination sites, enhancing alkyne partial hydrogenation.

In our work, the high density of surface functionalities on GO gives rise to a strong anchoring effect and thus produces thermodynamically nonequilibrium particle shapes at appro-

dx.doi.org/10.1021/cs5002724 | ACS Catal. 2014, 4, 2369−2373

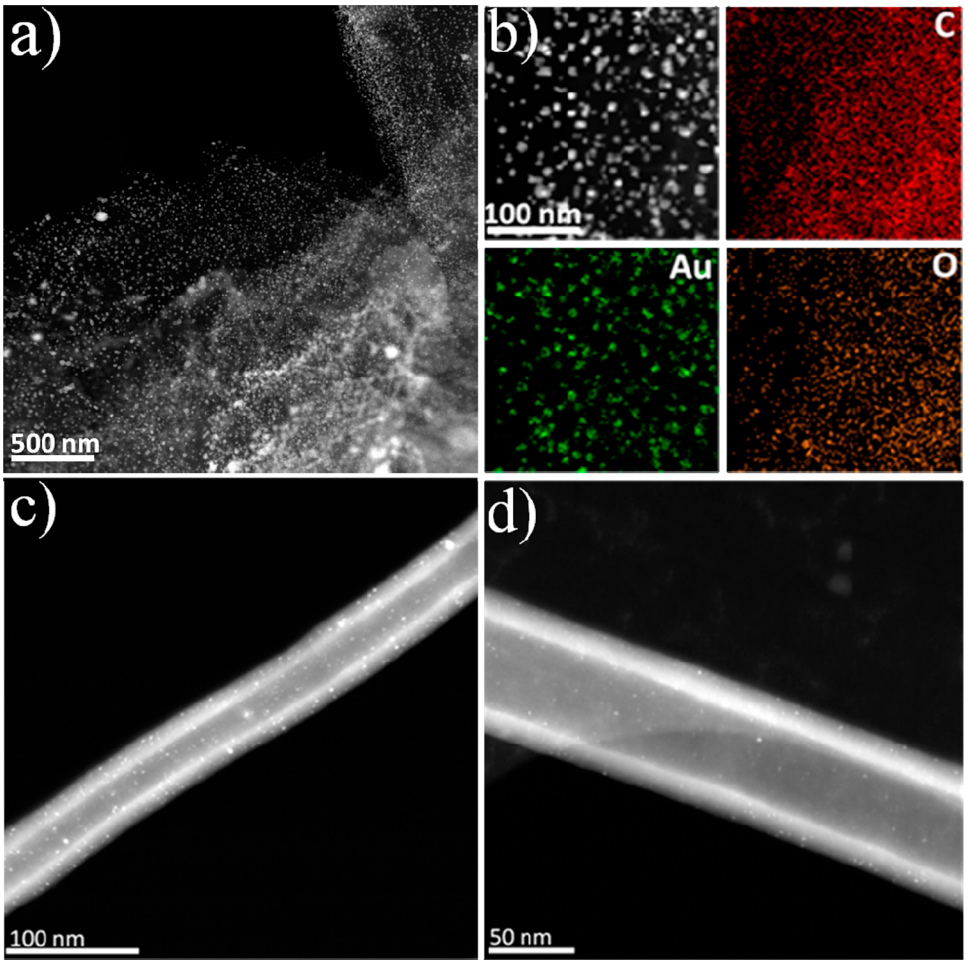

Figure 3. (a) STEM image revealing the Au dispersion of the used Au/GO. (b) STEM image and the corresponding STEM-EDX maps of C/Au/O of AuNPs supported on GO after reaction. (c) STEM image of fresh Au/CNTs. (d) STEM image of the used Au/CNTs.

priate reduction temperatures. On the other hand, the somewhat lower functionalization of CNTs allowed for gold–gold interaction and clustering during reductions in sample preparation. Thus, twinning occurred while particles were grown on CNTs. Accordingly, Au/CNTs exhibited lower activities in phenylacetylene hydrogenation compared to Au/GO under the same conditions.

In the AuNPs applications, oxidized species are commonly reported as coexisting species for influencing catalytic performance.[21] Oxidized Au species may be present on the surface before reductive treatment. Furthermore, preabsorbed species may influence catalytic applications by affecting surface-adsorbing strength toward other reactant molecules.[3,22] Therefore, sufficient reduction is required for obtaining the metallic phase of gold. However, special care during reduction process is necessary, because prolonged reduction time may lead to an increased twinning of AuNPs (Figure 2b). AuNP mean size was observed to increase to 18.6 ± 0.2 nm due to the progressive removal of functionalities under reductive atmosphere with prolonged reduction time. Tested in phenylacetylene hydrogenation, Au/GO after prolonged reduction exhibited significantly lower activity and styrene selectivity under the same conditions. The purpose of carrying out prolonged reduction and testing in hydrogenation was to prove the role of functionalities in affecting catalysis by influencing the geometrical structures of supported AuNPs.

Au/GO has not only exhibited enhanced activities and selectivities but also a high stability after several running cycles in flow reactor. To reach an understanding of the obtained high stability of Au/GO, used Au/GO was compared to fresh samples. Because no filtration is required for collecting or separating used catalyst from the reactant solution, running reactions in continuous flow aids a friendly platform for sample analysis. Another important character of using flow system is the continuous flow reaction pathway. In batch systems, leached metal particles can be reabsorbed onto the support surface during catalytic reaction.[23] As for in the flow system, such readsorption is unlikely taking place due to the one-direction sample scouring with continuous flows. Thus, the catalytic stability can be directly related to the information obtained on collected catalysts. The STEM imaging of used Au/GO (Figure 3a) suggests that the AuNPs retained a good dispersion with the mean size of 5.3 ± 0.2 nm (Figure S6 in SI). GO displays a similar morphology with no obvious surface and structural alternations compared to fresh Au/GO in Figure S4 in SI. Consistent with Figure 3a, a local view using the STEM-EDX mode displays a homogeneous distribution of Au, O, and C elements indicating the well-dispersed status, as seen in Figure 3b. Confirmed by X-ray fluorescence analysis (XFA), Au loading remained the same after hydrogenation. As for Au/CNTs, leaching of AuNPs was observed, as deduced from Figure 3d, in comparison to the fresh catalyst (Figure 3c). Confirmed by XFA, 0.4 wt % of Au loading was leached from

dx.doi.org/10.1021/cs5002724 | ACS Catal. 2014, 4, 2369–2373

the CNTs surface. Compared to Au/CNTs, the preservation of AuNPs on GO further confirmed the role of support by anchoring AuNPs. Thereby, a high stability toward selective phenylacetylene hydrogenation was achieved over Au/GO.

The role of functionalization of carbon supports in affecting hydrogenation was assessed by comparing Au/GO with Au/CNTs and Au/GO after prolonged reduction treatment. The XPS analysis revealed a higher functionalization profile on GO than on oxidized CNTs, suggesting that GO was advantageous in possessing more abundant functional groups that could serve as nucleation and anchored sites for nanoparticle growth. After metal ions coordinated with oxygen functional groups, hydrolysis is applied to crystallize the precursors nucleated on the oxidized carbon supports to form nanocrystals. The temperature and reduction time can tune the size, shape, and crystallinity of the nanocrystals. Small gold nanoparticles with nonequilibrium particle shape and exposing a large number of low coordination sites are crucial for both dissociative hydrogen activation and phenylacetyelene adsorption. Designing a strongly coupled AuNPs−GO hybrid material with optimal geometrical structure of gold nanoparticles is the key factor for improved hydrogenation performance.

In this work, gold was supported on GO and utilized in a hydrogenation application. A 99% styrene selectivity with a 99% conversion in the hydrogenation of phenylacetylene was obtained at 60 °C, which is far lower than the optimal temperature in most previous reports. Such catalytic performance was achieved in both continuous flow and batch systems over highly dispersed Au^0 nanoparticles on GO. In the flow system, Au/GO exhibited stable performance during several running cycles. Compared to Pd-based catalysts, the enhanced selectivities obtained over Au/GO were interpreted by the absence of the subsurface dynamics of metallic phase under reactive atmosphere and the preference for the desorption of partial hydrogenation product. Highly dispersed rounded AuNPs with enriched low-coordination sites were active and selective for phenylacetylene hydrogenation. These sites are crucial for both hydrogen activation and alkyne adsorption. The established correlation between the shape of AuNPs and improved catalytic performance demonstrated the influence of support functionalization on the geometrical structure of supported AuNPs. Prolonged reduction treatment further confirmed the support effect of GO on the shape and size of the AuNPs. Functionalized surfaces of GO synthesized from expanding and oxidizing graphite layers can hinder Au−Au interaction during catalyst preparation and tune the geometrical structures of thus formed AuNPs, retard thermal dynamics (crystalline changes, thermal aging, and leaching) of supported AuNPs under reaction conditions, and enhance the catalytic stability through metal−support interaction.

■ ASSOCIATED CONTENT

Supporting Information

Experimental procedures including material synthesis, electron microscopy, in situ X-ray photoelectron spectroscopy, and catalysis. This material is available free of charge via the Internet at http://pubs.acs.org.

■ AUTHOR INFORMATION

Corresponding Author

*E-mail: lidongshao@outlook.com.

Notes

The authors declare no competing financial interest.

■ REFERENCES

(1) Borodziński, A.; Bond, G. C. *Catal. Rev. Sci. Eng.* **2006**, *48*, 91−144.
(2) Molnár, Á.; Sárkány, A.; Varga, M. *J. Mol. Catal. A: Chem.* **2001**, *173*, 185−221.
(3) Shao, L. D.; Zhang, B. S.; Zhang, W.; Teschner, D.; Girgsdies, F.; Schlögl, R.; Su, D. S. *Chem.—Eur. J.* **2012**, *18*, 14962−14966.
(4) Teschner, D.; Borsodi, J.; Wootsch, A.; Révay, Z.; Havecker, M.; Knop-Gericke, A.; Jackson, S. D.; Schlögl, R. *Science* **2008**, *320*, 86−89.
(5) Green, I. X.; Tang, W. J.; Neurock, M.; Yates, J. T. *Science* **2011**, *333*, 736−739.
(6) Boronat, M.; Corma, A. *Langmuir* **2010**, *26*, 16607−16614.
(7) Corma, A.; Boronat, M.; González, S.; lllas, F. *Chem. Commun.* **2007**, 3371−3373.
(8) Nikolaev, S. A.; Krotova, I. N. *Petro. Chem.* **2013**, *53*, 394−400.
(9) Segura, Y.; López, N.; Pérez-Ramírez, J. *J. Catal.* **2007**, *247*, 383−386.
(10) Nikolaev, S. A.; Smirnov, V. V. *Catal. Today.* **2009**, *147*, S336−S341.
(11) Fletcher, J. C. Q.; Robert, S.; Julius, M.; McEwan, L. *Gold Bull.* **2010**, *43*, 298−306.
(12) Keane, M. A.; Cárdenas-Lizana, F. *J. Mater. Sci.* **2013**, *48*, 543−564.
(13) Derrien, M. L. In *Studies of Surface Science and Catalysis*; Cerveny, L., Ed.; Elsevier: Amsterdam, 1986; Vol. *27*, pp 613−665.
(14) Teschner, D.; Révay, Z.; Borsodi, J.; Havecker, M.; Knop-Gericke, A.; Schlögl, R.; Milroy, D.; Jackson, S. D.; Torres, D.; Sautet, P. *Angew. Chem., Int. Ed.* **2008**, *47*, 9274−9278.
(15) Shao, L. D.; Zhang, W.; Armbrüster, M.; Teschner, D.; Girgsdies, F.; Zhang, B. S.; Timpe, O.; Friedrich, M.; Schlögl, R.; Su, D. S. *Angew. Chem., Int. Ed.* **2011**, *50*, 10231−10235.
(16) Sheth, P. A.; Neurock, M.; Smith, C. *J. Phys. Chem. B* **2005**, *109*, 12449−12466.
(17) Shao, L. D.; Zhang, B. S.; Zhang, W.; Hong, S. Y.; Schlögl, R.; Su. *Angew. Chem., Int. Ed.* **2013**, *52*, 2114−2117.
(18) Sljivancanin, Z.; Hammer, B. *Phys. Rev. B* **2002**, *65*, 085414−1−085414−4.
(19) Hammer, B.; Nørskov, J. K. *Adv. Catal.* **2000**, *45*, 71−129.
(20) Hammer, B. *Top. Catal.* **2006**, *37*, 3−16.
(21) Hashmi, A. S. K. *Angew. Chem., Int. Ed.* **2005**, *44*, 6990−6993.
(22) Rinaldi, A.; Tessonnier, J. P.; Schuster, M. E.; Blume, R.; Girgsdies, F.; Zhang, Q.; Jacob, T.; Hamid, S. B. A.; Su, D. S.; Schlögl, R. *Angew. Chem., Int. Ed.* **2011**, *50*, 3313−3317.
(23) Phan, N. T. S.; Van Der Sluys, M.; Jones, C. W. *Adv. Synth. Catal.* **2006**, *348*, 609−679.